Article

Not peer-reviewed version

Optical Evaluation of Dansyl Derivatives and Their Implementation in Low-Cost and Flexible Dye-Doped PMMA Platforms for Efficient Detection of Hazardous Chemical Vapours

Gonçalo Pedro , Frederico Duarte , Georgi Dobrikov , Atanas Kurutos * , Hugo M Santos ,
José Luis Capelo-Martínez , Elisabete Oliveira * , Carlos Lodeiro *

Posted Date: 19 December 2023

doi: 10.20944/preprints202312.1441.v1

Keywords: Dansyl derivatives; Fluorescent Chemosensors; dye-doped PMMA polymers; Solvatochromic Properties

Article

Optical Evaluation of Dansyl Derivatives and Their Implementation in Low-Cost and Flexible Dye-Doped PMMA Platforms for Efficient Detection of Hazardous Chemical Vapours

Gonçalo Pedro [1], Frederico Duarte [1], Georgi M. Dobrikov [2,*], Atanas Kurutos [2,3], Hugo M. Santos [1,4], Jose Luis Capelo-Martinez [1,4], Elisabete Oliveira [1,4,*] and Carlos Lodeiro [1,4,*]

[1] BIOSCOPE Research Group, LAQV-REQUIMTE, Chemistry Department, NOVA School of Science and Technology, FCT NOVA, Universidade NOVA de Lisboa, 2829-516 Caparica, Portugal
[2] Institute of Organic Chemistry with Centre of Phytochemistry, Bulgarian Academy of Sciences, Acad. G. Bonchev str., bl. 9, 1113 Sofia, Bulgaria
[3] University of Chemical Technology and Metallurgy, 8 St. Kliment Ohridski blvd, 1756 Sofia, Bulgaria
[4] ROTEOMASS Scientific Society, BIOSCOPE Research Group, Departamental Building, Ground floor Caparica Campus, 2829-516 Caparica, Portugal.
* Correspondence: Georgi.Dobrikov@orgchm.bas.bg (GD); ej.oliveira@fct.unl.pt (EO) and cle@fct.unl.pt (CL)

Abstract: This study focuses on the development and characterization of a series of six new dansyl derivatives (**L1** to **L6**) and their integration into PMMA polymers for application in environmental sensing. The photophysical properties of these derivatives were extensively studied in various solvents and in solid state. A remarkable positive solvatochromic effect was observed, indicating their potential in microenvironmental polarity assessment. The dansyl derivatives demonstrated selective sensing capabilities for Cu^{2+} and Hg^{2+} metal ions, with the formation of mononuclear species. Additionally, their acid-base responsive nature was explored, revealing potential for pH-sensitive applications. The incorporation of these derivatives into PMMA polymers resulted in acid-base sensitive materials suitable for environmental monitoring, particularly in detecting hazardous gases and changes in pH levels. This integration overcomes the solubility limitations of dansyl compounds and extends their applicability in diverse sensing scenarios.

Keywords: dansyl derivatives; Fluorescent Chemosensors; dye-doped PMMA polymers; Solvatochromic Properties; Acidic Vapours Detection

1. Introduction

Over the past decade, there has been a significant focus on the design of fluorescent chemosensors due to their highly sensitive, rapid, and non-destructive analysis [1,2]. One of the commonly used fluorophores in this field is the dansyl group, which offers several advantages; it exhibits emission in the visible region, possesses an exceptionally high fluorescence quantum yield, and exhibits a significant Stokes shift, thereby avoiding any auto-absorption effects. These compounds incorporated electron-donating and electron-withdrawing moieties, which contribute to their high fluorescence quantum yields.

Furthermore, the fluorescence intensity and emission maximum of dansyl-based compounds are known to vary with the polarity of the surrounding environment, primarily due to their charge transfer properties being very useful for biological applications [3–6].

Based on the reports published in the literature [1,7,8], dansyl derivatives have demonstrated selective detection capabilities for Cu(II) and Hg(II) metal ions, as well as certain anions. These favourable properties make them highly relevant in fields such as environmental monitoring, bioanalytical chemistry, and clinical diagnostics. The advantage of dansyl-based compounds lies in

Preprints (www.preprints.org) | NOT PEER-REVIEWED | Posted: 19 December 2023 doi:10.20944/preprints202312.1441.v1

their ability to provide tailored selectivity, allowing for precise and reliable detection of these target analytes even in complex matrices.

However, it is worth noting that one restriction of dansyl derivatives is their limited solubility in water, which can hinder their application in biological and environmental contexts where aqueous environments are prevalent. The hydrophobic nature of these compounds restricts their dispersion and interaction with aqueous samples, thereby limiting their effectiveness as probes in such settings.

To overcome this limitation and expand the applicability of dansyl-based compounds in biological and environmental applications, researchers have explored various strategies. One such strategy is namely the incorporation of dansyl derivatives into polymers. This approach involves the synthesis or modification of polymers to include dansyl groups, thereby improving the solubility and dispersibility of the compounds in aqueous media.

The incorporation of dansyl derivatives into polymers offers multiple advantages and applications. Firstly, it provides a solid platform for immobilizing the probes, allowing for easy handling and practical use. The solid-state nature of polymer-based systems also enhances stability, which is essential for long-term sensing applications. Additionally, polymers can be tailored to have specific properties such as biocompatibility or environmental resistance, further expanding the range of applications for dansyl-based probes.

Thus, by incorporating dansyl derivatives into polymers, researchers can overcome the solubility limitation and create a robust sensing platform that retains their selective detection properties. This strategy not only improves the practicality of these compounds but also enables their use in various biological and environmental sensing applications, where stability, ease of use, and compatibility with different media are crucial considerations.

A thorough examination of the available literature reveals that polymers, alongside other materials, have also emerged as key materials in various gas sensor devices offering a promising and cost-effective solution for addressing issues related to hazardous gases in the environment. Conducting polymers has demonstrated remarkable applications in sensing gases with acid-base or oxidizing characteristics. Furthermore, when combined with other polymers like PVC and PMMA, which possess active functional groups capable of detecting such gases, they have shown significant potential [9]. Legislative measures have encouraged a substantial demand for sensors used in environmental monitoring, such as the detection of toxic gases and vapours in workplaces and contaminants in natural waters originating from industrial effluents and agricultural runoff.

In this study, a series of six new dansyl derivatives (**L1** to **L6**) were synthesized and thoroughly characterized. The photophysical properties of all compounds were investigated in various solvents, including DMSO, CH_3CN, ethanol, THF, and $CHCl_3$. To comprehensively explore the diverse characteristics of these compounds, they were primarily investigated for their solution-based properties, particularly the ability to sense metal ions. Additionally, these compounds were incorporated into PMMA polymers as sensing elements to detect acidic and basic environmental conditions on solid supports.

2. Materials and Methods

Reagents and solvents employed for the synthesis and purification of the target compounds (see Schemes 1–3) were available with purity >98% and purchased from Fluorochem, Sigma-Aldrich or TCI: 2-aminobenzoic acid (**1**), thiomorpholine (**2**), thiophen-2-ylmethanamine (**3**), thiophene-2-sulfonyl chloride (**7**), 2-(aminomethyl)aniline (**6**), 5-(dimethylamino)naphthalene-1-sulfonyl chloride (dansyl chloride) (**9**), methyl isothiocyanate (MeNCS), 2-(methylthio)aniline (**10**), 2-(1*H*-Benzotriazole-1-yl)-1,1,3,3-tetramethylaminium tetrafluoroborate (TBTU), *N*-Ethyldiisopropylamine (DIPEA), triethylamine (Et_3N), pyridine, methanol (MeOH), methyl tert-butyl ether (MTBE) and dichloromethane (DCM). Reagents and solvents required for the photophysical experiments: acetonitrile (CH_3CN) (Merck Millipore, Darmstadt, Germany, 99.5%, CAS 75-05-8); chloroform ($CHCl_3$) (Honeywell, Minneapolis, MN, USA, 99.0–99.4%, CAS 67-66-3); diemthylsulfoxyde (DMSO) (Honeywell, 99.5%, CAS 67-68-5); ethanol (EtOH) (Honeywell, 99.9%, CAS 64-17-5); tetrahydrofuran (THF) (PanReac, Barcelona, Spain, 99.0%, CAS 109-99-9); acetone (Honeywell, 99.5%, 67-64-1);

Preprints (www.preprints.org) | NOT PEER-REVIEWED | Posted: 19 December 2023 doi:10.20944/preprints202312.1441.v1

ethylenediamine tetraacetic acid (EDTA) (Alfa Aesar, Ward Hill, MA, USA, CAS 194491-31-1); LUDOX® AS-30 colloidal silica (SiO_2, Sigma-Aldrich, 30 wt.% suspension in water, CAS 7631-86-9); poly(methyl methacrylate) (PMMA) (Sigma-Aldrich, St, Louis, MO, USA, MW ~350,000, CAS 9011-14-7); Zinc (II) trifluoromethanesulfonate (Sigma-Aldrich, St, Louis, MO, USA, CAS 54010-75-2); Silver (I) trifluoromethanesulfonate (Sigma-Aldrich, St, Louis, MO, USA, CAS 2923-28-6); Mercury (II) trifluoromethanesulfonate (Sigma-Aldrich, St, Louis, MO, USA, CAS 49540-00-3); Copper (II) trifluoromethanesulfonate (Sigma-Aldrich, St, Louis, MO, USA, CAS 34946-82-2); Acridine Yellow G (Sigma-Aldrich, St, Louis, MO, USA, CAS 135-49-9); hydrochloric acid 37% (Honeywell, CAS 7647-01-0); ammonia (Sigma-Aldrich, St, Louis, MO, USA, CAS 7664-41-7); H_2O (Milli-Q ultrapure).

The absorption spectra were recorded on a JASCO V-650 UV-Vis Spectrophotometer and the fluorescence emission spectra on a Horiba Jobin-Yvon Scientific Fluoromax-4. Spectra of solid samples were collected with a Horiba-Jobin-Yvon Fluoromax-4® spectrofluorometer using an optic fibre connected to the equipment, by exciting the solid compounds at appropriated λ (nm). A correction for the absorbed light was performed when necessary. Lifetime studies were carried out on TemPro, Deltahub Nanoled of Horiba Jobin-Yvon, with a 390 nm Nanoled. All instruments were provided by Proteomass-BIOSCOPE facility.

The chemical identities of all substances were confirmed through the utilization of various analytical techniques, including ^{1}H NMR, ^{13}C NMR, 2-D COSY, 2D-HSQC, and 2-D HMBC techniques. The ^{1}H NMR and ^{13}C NMR spectra were acquired on a Bruker Avance II$^+$ 600 spectrometer using 5 mm tubes. The measurements were performed in $CDCl_3$ and DMSO-d_6 at a temperature of 293 K, with operating frequencies of 600.13 MHz and 150.92 MHz for ^{1}H and ^{13}C nuclei, respectively. The ^{1}H and ^{13}C nuclear magnetic resonance (NMR) spectra were standardized using the reference signal of tetramethylsilane (TMS) with a chemical shift value (δ) of 0.00. The precision of chemical changes is determined at a level of 0.01 ppm. The coupling constants (*J*) are displayed with a precision of 0.1 and denoted in units of hertz (Hz). The spin multiplicity observed in the ^{1}H nuclear magnetic resonance (NMR) spectroscopy was represented using the following abbreviations: s for singlet, d for doublet, t for triplet, q for quartet, dd for doublet of doublets, dt for doublet of triplets, td for triplet of doublets, and m for multiplet. MestreNova v. 14.1.1 (Mestrelab Research S.L.) was used for processing the spectra.

High-Resolution Mass Spectrometry analyses were carried out in the Laboratory for Biological Mass Spectrometry–Isabel Moura (PROTEOMASS Scientific Society Facility), using UHR ESI-Qq-TOF IMPACT HD (Bruker-Daltonics, Bremen, Germany). Compounds were dissolved in 50% (v/v) Acetonitrile containing 0.1% (v/v) aqueous formic acid to obtain a working solution of 0.1 µg/mL. Mass spectrometry analysis was carried out by the direct infusion of the compound solutions into the ESI source. MS data were acquired in positive polarity over the mass range of 80 – 1300 m/z. (Capillary voltage: 4500 V, End plate offset: -500 V, Charging voltage: 2000 V, Corona: 4000 nA, Nebulizer gas: 0.4 Bar, Dry Heater: 180 ºC, Dry gas: 4.0 L/min).

2.1. Synthetic procedures

2.1.1. Synthetic procedures for intermediates 4, 5, 8 and 12.

Synthesis of (2-aminophenyl)(thiomorpholino)methanone (**4**):

To a solution of aminoacid **1** (0.500 g, 3.65 mmol, 1.1 eq.) in 25 mL dry DCM were added at r.t. consequently DIPEA (1.21 mL, 7.29 mmol, 2.2 eq.), thiomorpholine **2** (0.33 mL, 3.31 mmol, 1.0 eq.) and TBTU (1.170 g, 3.65 mmol, 1.1 eq.). The formed clear solution was stirred at r.t. for 24 h. Workup: reaction mixture was diluted with 40 mL DCM and consequently washed with aq. K_2CO_3 (x1) and water (x2). TLC – DCM:MTBE=5:1, x2. Organic phase was dried over anhydr. Na_2SO_4 and evaporated *in vacuo* to dryness. The crude product was purified employing column chromatography: 40 g silica, mobile phase DCM:MTBE=10:1, furnishing0.700 g (96%) of compound **4** as pale yellow solid. ^{1}H NMR (600 MHz, $CDCl_3$) δ 7.17 (m, 1H), 7.05 (dd, J = 7.8, 1.6 Hz, 1H), 6.70-6.74 (m, 2H), 3.86 (br s, 4H), 2.66

3.86 (br s, 4H). ^{13}C NMR (151 MHz, $CDCl_3$) δ 170.32 (1C, C=O), 145.40, 130.70, 127.48, 119.73, 117.62, 116.80, 27.88.

Synthesis of 2-amino-*N*-(thiophen-2-ylmethyl)benzamide (**5**):

To a solution of aminoacid **1** (0.400 g, 2.92 mmol, 1.0 eq.) in 25 mL dry DCM were added at r.t. consequently DIPEA (1.21 mL, 7.29 mmol, 2.5 eq.), amine **3** (0.33 mL, 3.21 mmol, 1.1 eq.) and TBTU (1.030 g, 3.21 mmol, 1.1 eq.). The formed clear solution was stirred at r.t. for 24 h. Workup: reaction mixture was diluted with 40 mL DCM and washed consequently with aq. citric acid and water. TLC – DCM, x2. The organic phase was dried over anhydr. Na_2SO_4 and evaporated *in vacuo* to dryness. The crude product was purified by column chromatography: 40 g silica, mobile phase DCM, affording 0.580 g (86%) of compound **5** as a white solid. M.p. 111-112°C. ^{1}H NMR (600 MHz, $CDCl_3$) δ 7.30 (dd, *J* = 7.9, 1.4 Hz, 1H), 7.24 (dd, *J* = 5.1, 1.1 Hz, 1H), 7.20 (ddd, *J* = 8.5, 7.2, 1.5 Hz, 1H), 7.02 (m, 1H), 6.97 (dd, *J* = 5.1, 3.5 Hz, 1H), 6.68 (dd, *J* = 8.1, 0.9 Hz), 6.62 (ddd, *J* = 8.1, 7.3, 1.1 Hz, 1H), 6.40 (br s, 1H, CO-NH), 5.54 (br s, 2H, NH_2), 4.76 (dd, *J* = 5.6, 0.6 Hz, 2H, CH_2). ^{13}C NMR (151 MHz, $CDCl_3$) δ 168.93 (1C, C=O), 148.85, 140.94, 132.50, 127.16, 126.93, 126.08, 125.30, 117.32, 116.58, 115.48, 38.47 (1C, CH_2).

Synthesis of *N*-(2-aminobenzyl)thiophene-2-sulfonamide (**8**):

Diamine **6** (0.304 g, 2.49 mmol, 1.0 eq.) was dissolved in 25 mL dry DCM and Et_3N (0.42 mL, 2.99 mmol, 1.2 eq.) was added. The formed clear solution was cooled down to 5°C (with water-ice) and sulfochloride **7** (0.500 g, 2.74 mmol, 1.1 eq.) was added portionwise. The resulting clear reaction mixture was stirred for 30 min at 5°Cfollowed by 20 h at r.t. Workup: the reaction mixture was diluted with 40 mL DCM and consequently washed with aq. citric acid and water. TLC – DCM, x2. The organic phase was dried over anhydr. Na_2SO_4 and evaporated *in vacuo* to dryness. The crude product was purified by column chromatography: 40 g silica, mobile phase DCM:MTBE=20:1, to yield 0.670 g (99%) of compound **8** as white solid. M.p. 132-133°C. ^{1}H NMR (600 MHz, $CDCl_3$) δ 7.62-7.66 (m, 2H), 7.10-7.14 (m, 2H), 6.93 (dd, *J* = 7.4, 0.9 Hz, 1H), 6.64-6.69 (m, 2H), 4.70 (t, *J* = 5.7 Hz, 1H, SO_2-NH), 4.10 (d, *J* = 6.2 Hz, 2H, CH_2), 4.03 (br s, 2H, NH_2). ^{13}C NMR (151 MHz, $CDCl_3$) δ 145.62, 139.93, 132.60, 132.31, 130.30, 129.88, 127.60, 119.16, 118.26, 116.28, 45.70 (1C, CH_2).

Synthesis of *N*-(2-aminobenzyl)-5-(dimethylamino)naphthalene-1-sulfonamide (**12**):

To a solution of diamine **6** (0.400 g, 3.27 mmol, 1.0 eq.) in 25 mL dry DCM was added at r.t. Et_3N (0.59 ml, 4.26 mmol, 1.3 eq.). The formed clear solution was cooled to 5°C (with water-ice) and dansyl chloride **9** (0.972 g, 3.60 mmol, 1.1 eq.) was added in portions. The formed clear yellow solution was stirred for 1 h at 5°C, followed by20 h at r.t. Workup: reaction mixture was diluted with 40 mL DCM and washed with water. TLC – DCM:MTBE=50:1, x2. The organic phase was dried over anhydr. Na_2SO_4 and evaporated *in vacuo* to dryness. The crude product was purified by column chromatography: 60 g silica; mobile phase DCM:MTBE=50:1, affording 1.170 g (99%) of compound **12** as bright yellow solid. ^{1}H NMR (600 MHz, $CDCl_3$) δ 8.56 (m, 1H), 8.29 (dd, *J* = 7.3, 1.2 Hz, 1H), 8.26 (m, 1H), 7.52-7.57 (m, 2H), 7.19 (br d, *J* = 7.5 Hz, 1H), 7.04 (dt, *J* = 7.7, 1.4 Hz, 1H), 6.78 (dd, *J* = 7.9, 1.4 Hz, 1H), 6.55-6.58 (m, 2H), 4.87 (t, *J* = 6.1 Hz, 1H, SO_2NH), 3.93 (br s, 1H, NH_2), 3.91 (d, *J* = 6.1 Hz, 2H, CH_2), 2.90 (s, 6H, NMe_2). ^{13}C NMR (151 MHz, $CDCl_3$) δ 152.11, 145.57, 133.78, 130.79, 130.26, 130.18, 129.84, 129.63, 129.54, 128.62, 123.28, 119.50, 118.30, 118.06, 116.12, 115.25, 45.47 (1C, CH_2), 45.41 (2C, NMe_2).

2.1.2. Synthetic procedures for target compounds L1-L6

Synthesis of 5-(dimethylamino)-*N*-(thiophen-2-ylmethyl)naphthalene-1 sulfonamide (**L1**):

To a solution of amine **3** (0.17 mL, 1.63 mmol, 1.1 eq.) in 20 mL dry DCM was added at r.t. DIPEA (0.31 mL, 1.78 mmol, 1.2 eq.). The formed clear solution was cooled down to 5°C (with water-ice) and dansyl chloride **9** (0.400 g, 1.48 mmol, 1.0 eq.) was added in portions. The resulting clear yellow solution was stirred for 1 h at 5°C, followed by24 h at r.t. Workup: reaction mixture was diluted with

Preprints (www.preprints.org) | NOT PEER-REVIEWED | Posted: 19 December 2023 doi:10.20944/preprints202312.1441.v1

40 mL DCM and consequently washed with aq. citric acid and water. TLC – DCM, x2. Organic phase was dried over anhydr. Na_2SO_4 and evaporated *in vacuo* to dryness. The crude product was purified by column chromatography: 70 g silica; mobile phase DCM. After column purification, the product was washed with 3 mL of hot petroleum ether, cooled down to r.t., decanted and dried *in vacuo* to give 0.480 g (93%) of pure **L1** as pale-yellow powder. M.p. 113-114°C. 1H NMR (600 MHz, CDCl3) δ 8.54 (dt, *J* = 8.5, 1.1 Hz, 1H), 8.26 (tt, *J* = 7.1, 1.1 Hz, 2H), 7.56 (dd, *J* = 8.6, 7.5 Hz, 1H), 7.52 (dd, *J* = 8.5, 7.2 Hz, 1H), 7.19 (dd, *J* = 7.6, 0.9 Hz, 1H), 7.09 (dd, *J* = 5.1, 1.2 Hz, 1H), 6.77 (dd, *J* = 5.1, 3.5 Hz, 1H), 6.72 (dt, *J* = 3.5, 1.0 Hz, 1H), 4.94 (t, *J* = 6.0 Hz, 1H), 4.28 (dd, *J* = 6.2, 0.9 Hz, 2H), 2.90 (s, 6H). 13C NMR (151 MHz, CDCl3) δ 152.02, 138.72, 134.37, 130.69, 129.87, 129.60, 128.52, 126.69, 126.47, 125.72, 123.15, 118.58, 115.19, 77.23, 77.02, 76.81 (Figures S1-1 to S1-18). ESI-MS: $[M+H]^+$ for $C_{17}H_{19}N_2O_2S_2$ = 347.0882 (-0.1 ppm). Calculated $[M+H]^+$ for $C_{17}H_{19}N_2O_2S_2$ = 347.088246.

Synthesis of 5-(dimethylamino)-*N*-(2-(thiomorpholine-4 carbonyl)phenyl)naphthalene-1-sulfonamide (**L2**):

To 10 mL dry pyridine was added intermediate **4** (0.700 g, 3.15 mmol, 1.0 eq.) and dansyl chloride **9** (1.020 g, 3.78 mmol, 1.2 eq.). The reaction mixture was gently refluxed at 115°C for 2 h (until exhaustion of **4**). TLC – DCM:MTBE=50:1, x2. Workup: reaction mixture was diluted with 70 mL DCM and consequently washed with aq. citric acid (x2) and water (x2). The organic phase was dried over anhydr. Na_2SO_4 and evaporated *in vacuo* to dryness. The crude product was purified by column chromatography: 60 g silica; mobile phase DCM:MTBE=50:1. After purification by column the product was washed with 3 mL hot petroleum ether, cooled down to r.t., decanted and dried *in vacuo* to give 1.000 g (70%) of compound **L2** as light-yellow powder. M.p. 176-177°C. 1H NMR (600 MHz, CDCl3) δ 8.68 (s, 1H), 8.50 (dt, *J* = 8.6, 1.1 Hz, 1H), 8.33 (dt, *J* = 8.6, 1.0 Hz, 1H), 8.13 (dd, *J* = 7.3, 1.3 Hz, 1H), 7.77 (dd, *J* = 8.4, 1.1 Hz, 1H), 7.63 (dd, *J* = 8.7, 7.5 Hz, 1H), 7.41 (dd, *J* = 8.5, 7.3 Hz, 1H), 7.34 (ddd, *J* = 8.6, 7.4, 1.6 Hz, 1H), 7.28 – 7.22 (m, 1H), 7.03 (td, *J* = 7.5, 1.2 Hz, 1H), 6.93 (dd, *J* = 7.7, 1.6 Hz, 1H), 3.50 (s, 2H), 2.88 (s, 6H), 2.69 (s, 2H), 2.46 (s, 2H), 2.02 (s, 2H).13C NMR (151 MHz, CDCl3) δ 168.58, 152.09, 136.08, 134.50, 131.04, 130.65, 130.09, 129.89, 129.23, 128.63, 127.16, 125.81, 124.27, 124.13, 123.18, 118.94, 115.71, 77.24, 77.03, 76.82, 45.49, 27.32 (Figures S2-1 to S2-13). ESI-MS: $[M+H]^+$ for $C_{23}H_{26}N_3O_3S_2$ = 456.1407 (-0.7 ppm). Calculated $[M+H]^+$ for $C_{23}H_{26}N_3O_3S_2$ = 456.141010.

Synthesis of 5-(dimethylamino)-*N*-(2-(methylthio)phenyl)naphthalene-1-sulfonamide (**L3**):

To 4 mL dry pyridine were added amine **10** (0.338 g, 2.43 mmol, 1.0 eq.) and dansyl chloride **9** (0.786 g, 2.91 mmol, 1.2 eq.). The reaction mixture was stirred at r.t for 48 h (until exhaustion of **10**). TLC – DCM:PE=1:1, x2. Workup: the reaction mixture was diluted with 50 mL DCM and consequently washed with 2N HCl and water. The organic phase was dried over anhydr. Na_2SO_4 and evaporated *in vacuo* to dryness. The crude product was purified by column chromatography: 70 g silica; mobile phase DCM. After column product was washed with 3 mL hot petroleum ether, cooled down to room temperature, decanted and dried *in vacuo* affording 0.640 g (70%) of compound **L3** as yellow powder. M.p. 101-102°C. 1H NMR (600 MHz, CDCl3) δ 8.50 (dt, *J* = 8.5, 1.1 Hz, 1H), 8.39 (dd, *J* = 8.7, 1.0 Hz, 1H), 8.29 (dd, *J* = 7.3, 1.3 Hz, 1H), 8.15 (s, 1H), 7.57 (dd, *J* = 8.7, 7.5 Hz, 1H), 7.51 – 7.44 (m, 2H), 7.32 (dd, *J* = 7.7, 1.6 Hz, 1H), 7.16 (dd, *J* = 7.6, 0.9 Hz, 1H), 6.93 (td, *J* = 7.6, 1.3 Hz, 1H), 2.84 (s, 6H), 2.03 (s, 3H). 13C NMR (151 MHz, CDCl3) δ 151.95, 137.89, 134.18, 134.10, 130.99, 130.39, 129.84, 129.47, 129.19, 128.55, 125.79, 124.35, 123.01, 118.69, 118.48, 115.27, 77.24, 77.02, 76.81, 45.38, 19.59 (Figures S3-1 to S3-12). ESI-MS: $[M+H]^+$ for $C_{19}H_{21}N_2O_2S_2$ = 373.1050 (3 ppm). Calculated $[M+H]^+$ for $C_{19}H_{21}N_2O_2S_2$ = 373.103896.

Synthesis of *N*-(2-((5-(dimethylamino)naphthalene)-1-sulfonamido)benzyl)thiophene-2-sulfonamide (**L4**):

To 10 mL dry pyridine were added intermediate **8** (0.300 g, 1.12 mmol, 1.0 eq.) and dansyl chloride **9** (0.362 g, 1.34 mmol, 1.2 eq.). The reaction mixture was gently refluxed at 115°C for 4 h (until exhaustion of **8**). TLC – DCM:PE=1:1, x2. Workup: the reaction mixture was diluted with 70 mL DCM and consequently washed with aq. citric acid (x3) and water (x2). Organic phase was dried over anhydrous Na_2SO_4 and evaporated *in vacuo* to dryness. The crude product was purified by column chromatography: 70 g silica; mobile phase DCM:MTBE=100:1. After column chromatography, the product was washed with 3 mL hot petroleum ether, cooled down to r.t., decanted and dried *in vacuo* to give 0.560 g (99%) of compound **L4** as yellow powder. M.p. 83-84°C. 1H NMR (600 MHz, CDCl3) δ 8.52 (dt, *J* = 8.5, 1.2 Hz, 1H), 8.31 (dd, *J* = 8.7, 1.0 Hz, 1H), 8.09 (dd, *J* = 7.3, 1.3 Hz, 1H), 7.63 (s, 1H), 7.62 (q, *J* = 1.4 Hz, 1H), 7.58 (dd, *J* = 8.7, 7.5 Hz, 1H), 7.43 (dd, *J* = 8.5, 7.3 Hz, 1H), 7.21 (s, 1H), 7.19 (dd, *J* = 7.7, 0.9 Hz, 1H), 7.17 (dd, *J* = 7.5, 1.7 Hz, 1H), 7.11 (dd, *J* = 4.9, 3.9 Hz, 1H), 7.04 (td, *J* = 7.5, 1.4 Hz, 1H), 6.99 (td, *J* = 7.7, 1.7 Hz, 1H), 6.72 (dd, *J* = 8.0, 1.4 Hz, 1H), 5.26 (t, *J* = 6.6 Hz, 1H), 4.07 (d, *J* = 6.6 Hz, 2H), 2.89 (s, 6H). 13C NMR (151 MHz, CDCl3) δ 152.07, 140.08, 134.79, 133.86, 132.59, 132.33, 131.00, 130.95, 130.72, 130.61, 129.70, 129.53, 129.17, 128.89, 127.61, 126.65, 124.69, 123.12, 118.50, 115.33, 77.23, 77.02, 76.81, 45.41, 44.27 (Figures S4-1 to S4-13). ESI-MS: $[M+H]^+$ for $C_{23}H_{24}N_3O_4S_3$= 502.0938 (2.9 ppm). Calculated $[M+H]^+$ for $C_{23}H_{24}N_3O_4S_3$ = 502.092346.

Synthesis of 5-(dimethylamino)-*N*-(2-(3-methylthioureido)benzyl)naphthalene-1-sulfonamide (**L5**):

A solution of **12** (0.410 g, 1.15 mmol, 1.0 eq.) and methyl isothiocyanate (0.168 g, 2.30 mmol, 2.0 eq.) in 10 mL dry MeOH was gently refluxed for 8 h (until exhaustion of **12**). TLC – DCM:MTBE=20:1, x2. Workup: the solvent was evaporated to dryness and the rest was purified using column chromatography: 60 g silica; mobile phase DCM:MTBE=20:1. After the column purification, the product was washed with 3 mL hot petroleum ether, cooled down to room temperature, decanted and dried *in vacuo* furnishing 0.400 g (81%) of compound **L5** as yellow powder. M.p. 99-100°C. 1H NMR (600 MHz, DMSO) δ 8.72 (s, 1H), 8.47 (dt, *J* = 8.5, 1.0 Hz, 1H), 8.36 (dt, *J* = 8.7, 0.9 Hz, 1H), 8.12 (dd, *J* = 7.3, 1.3 Hz, 1H), 7.95 (s, 1H), 7.58 (dd, *J* = 8.6, 7.4 Hz, 2H), 7.27 (dd, *J* = 7.5, 0.9 Hz, 2H), 7.19 (td, *J* = 7.6, 1.6 Hz, 1H), 7.12 (dd, *J* = 7.9, 1.4 Hz, 1H), 7.08 (td, *J* = 7.5, 1.4 Hz, 1H), 4.05 (s, 2H), 2.86 (d, *J* = 2.4 Hz, 9H). 13C NMR (151 MHz, DMSO) δ 182.37, 151.13, 135.94, 134.24, 128.98, 128.96, 128.88, 128.04, 127.76, 127.52, 127.34, 127.13, 125.85, 122.95, 118.79, 114.75, 44.63, 41.98, 30.70 (Figures S5-1 to S5-13). ESI-MS: $[M+H]^+$ for $C_{21}H_{25}N_4O_2S_2$= 429.1425 (2.7 ppm). Calculated $[M+H]^+$ for $C_{21}H_{25}N_4O_2S_2$= 429.141344.

Synthesis of 2-((5-(dimethylamino)naphthalene)-1-sulfonamido)-*N*-(thiophen-2-ylmethyl)benzamide (**L6**):

To 5 mL dry pyridine was added intermediate **5** (0.250 g, 1.08 mmol, 1.0 eq.) and dansyl chloride **9** (0.348 g, 1.29 mmol, 1.2 eq.). The reaction mixture was stirred at r.t for 48 h (until exhaustion of **5**). TLC – DCM, x2. Workup: the reaction mixture was diluted with 70 mL DCM and consequently washed with 2N HCl (x1) and water (x2). The organic phase was dried over anhydr. Na_2SO_4 and evaporated *in vacuo* to dryness. The crude product was purified by column chromatography: 70 g silica; phase DCM:MTBE=100:1. After column product was washed with 3 ml hot PE, cooled, decanted, and dried *in vacuo* yielding 0.350 g (70%) of compound **L6** as yellow powder. M.p. 210-211°C. 1H NMR (600 MHz, CDCl3) δ 11.18 (s, 1H), 8.48 (dt, *J* = 8.5, 1.2 Hz, 1H), 8.38 (d, *J* = 8.7 Hz, 1H), 8.26 (dd, *J* = 7.3, 1.3 Hz, 1H), 7.60 (dd, *J* = 8.4, 1.1 Hz, 1H), 7.55 (dd, *J* = 8.7, 7.6 Hz, 1H), 7.44 (dd, *J* = 8.5, 7.3 Hz, 1H), 7.29 (ddd, *J* = 8.6, 7.4, 1.5 Hz, 1H), 7.26 – 7.21 (m, 2H), 7.14 (d, *J* = 7.3 Hz, 1H), 6.96 (d, *J* = 3.4 Hz, 2H), 6.90 (td, *J* = 7.6, 1.1 Hz, 1H), 6.20 (t, *J* = 5.4 Hz, 1H), 4.55 (d, *J* = 5.5 Hz, 2H), 2.84 (s, 6H). 13C NMR (151 MHz, CDCl3) δ 167.89, 151.70, 139.60, 138.91, 134.63, 132.66, 130.69, 130.08, 129.76, 129.54, 128.37, 127.04, 126.63, 126.58, 125.63, 122.97, 122.83, 120.37, 119.94, 119.18, 115.25, 77.23, 77.02, 76.81, 45.41, 38.57 (Figures S6-1 to S6-16). ESI-MS: $[M+H]^+$ for $C_{24}H_{24}N_3O_3S_2$= 466.1253 (-0.1 ppm). Calculated $[M+H]^+$ for $C_{24}H_{24}N_3O_3S_2$ = 466.125360.

2.2.. Spectrophotometric and spectrofluorometric measurements

The spectroscopic characterizations and titrations were performed using stock solutions of the compounds (ca. 10^{-3} M), prepared by dissolving the appropriate amounts of each compound **L1**-**L6** in acetonitrile, chloroform, dimethyl sulfoxide, tetrahydrofuran, and ethanol. The studied solutions were prepared by appropriate dilution of the stock solutions up to 10^{-5}–10^{-6}. Titrations of compounds **L1**-**L6** were carried out in acetonitrile by the addition of microliter amounts of standard metal solutions of Zn^{2+}, Ag^{+}, Hg^{2+} and Cu^{2+} in acetonitrile and HCl and NH_3 in H_2O. The complexation constants for the interaction of ligands **L1** to **L6** in the presence of Hg^{2+} and Cu^{2+} metal ions were calculated using the HypSpec software [10].

Luminescence quantum yield of compounds **L1**-**L6** was measured using a solution of Acridine Yellow [φ = 0.37] [11,12] in ethanol as standard. All measurements were performed at 298 K.

2.3.. Dye doped PMMA Polymeric films

The doped polymer films were obtained at room temperature by dissolving 100 mg of PMMA in 5 mL of chloroform, followed by the addition of 1 mg of each compound **L1**-**L6**, previously dissolved in 1 mL of chloroform. The polymer films were obtained after slow evaporation at room temperature (24 h).

2.4. Acidity Assays

The reactivity and resistance of the dye-doped polymers to HCl and vapours were tested by dipping the polymer in a 2-12 M gradient and into vapours of concentrated HCl. The reproducibility of the dye-doped polymers was proved by continuous emersion of the polymers in HCl and ammonia for ten cycles. The changes in the polymers were spectroscopically analyzed.

3. Results and Discussion

3.1. Synthesis

A series of six dansyl derivatives **L1**-**L6** were prepared (Schemes 1–3), and their photophysical properties were examined in current investigation. According to databases, five of them are new. Only compound **L1** was obtained earlier, in a publication concerning the development of new method for the synthesis of sulfonamides from benzylic alcohols [13]. However, the photophysical properties of this compound were not subjected to further studies.

The synthesis of four intermediates **4**, **5** and **8** from commercially available reagents was performed (Scheme 1). These intermediate products were obtained quantitatively and used in the next steps for the synthesis of the target compounds. Compound **4** was prepared under basic conditions, through a reaction between anthranilic acid (**1**) and thiomorpholine in the presence of coupling reagent TBTU. Amide **5** was prepared in a similar manner from **1** and amine **3**. Amide **8** was obtained also by selective acylation of diamine **6** with sulfochloride **7** (Scheme 3). The coupling reactions occur selectively towards the aliphatic amino group, which is not unusual [14]. Thus, due to stronger nucleophilicity of aliphatic amino groups in reagents **2**, **3** and **6** there is no need for protection of the aromatic groups of **1** and **6**. Amides **4**, **5** and **8** were observed as single-step reaction products.

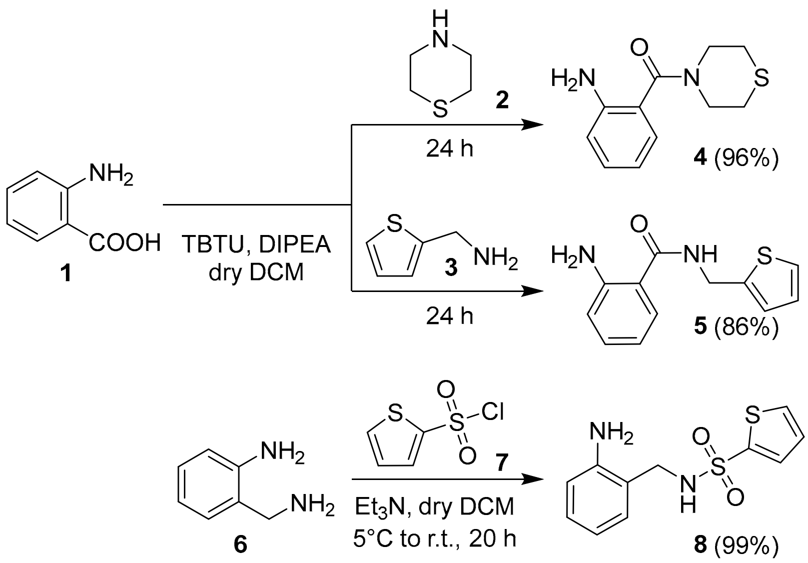

Scheme 1. Synthetic approach to the preparation of intermediates **4**, **5** and **8**.

Preprints (www.preprints.org) | NOT PEER-REVIEWED | Posted: 19 December 2023 doi:10.20944/preprints202312.1441.v1

Intriguingly, the preparation and structural characterization of **4** [15] and **5** [14,16–19] was already described in some studies. However, different synthetic methods were employed – aminolysis of isatoic anhydride with amines **2** and **3**, respectively. The preparation of intermediate **12** starting from commercially available dansyl chloride (**9**) and diamine **6** (Scheme 3) was performed by implementation of an existing protocol [20].

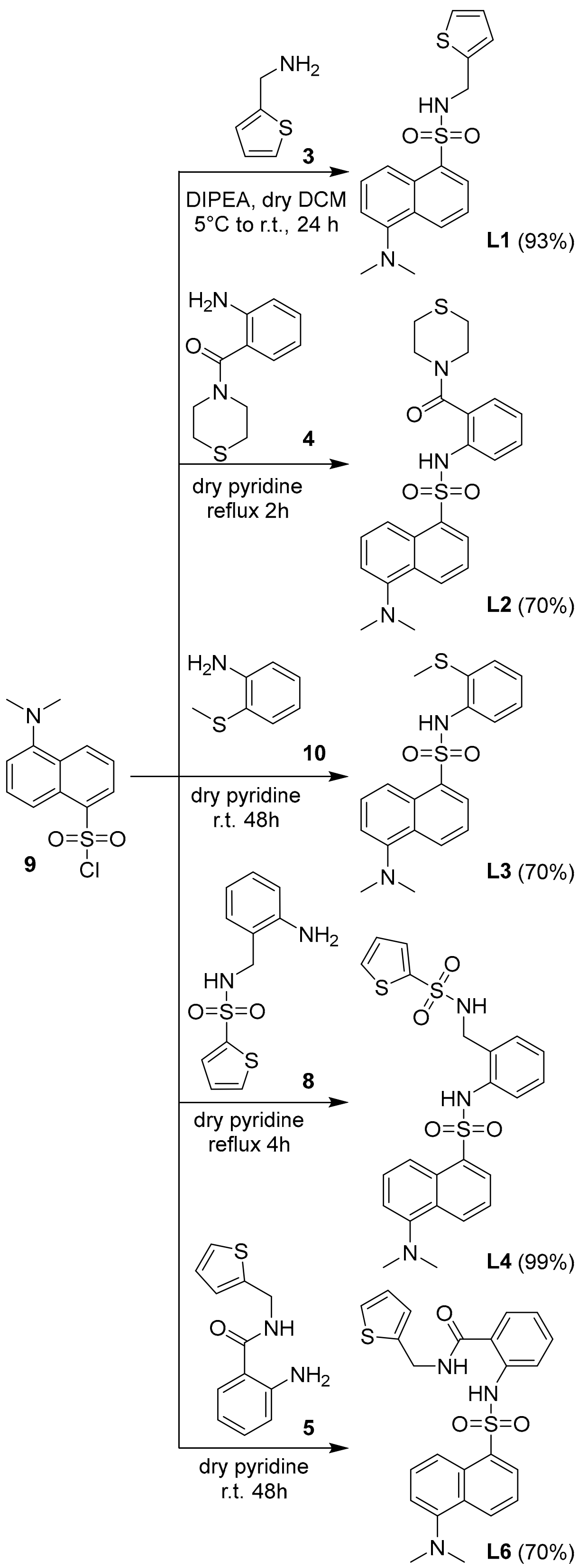

Scheme 2. Synthetic approach to the preparation of the target compounds **L1-L4** and **L6**.

The synthesis of amide **L1** (Scheme 2) was accomplished by one step acylation of amine **3** with **9** in the presence of DIPEA. Other target compounds (**L2-L4** and **L6**) were prepared by acylation of the above-mentioned intermediates (**4**, **5** and **8**) or the commercially available amine **10** with dansyl chloride (**9**) in dry pyridine. The reaction outcome was monitored using TLC until starting reagents exhausted. Compound **L5** was prepared by addition of methyl isothiocyanate to intermediate **12** in refluxing methanol (Scheme 3), as *Ambati et al.* described for similar compounds [21]. All target compounds **L1-L6** were obtained quantitatevely. Due to steric hindrance (as in the case of compound **L2**) or possible tautomerism (in the case of **L5**), NMR spectra of both compounds at room temperature were not enough informative. Thus, they were performed at 353 K aiming to obtain narrow signals.

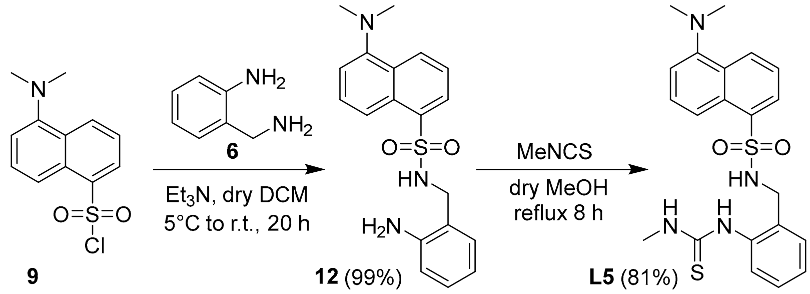

Scheme 3. Synthesis of intermediate **12** and target compound **L5**.

3.2. Photophysical studies

The absorption and emission spectra of all six dansyl derivatives **L1-L6** were studied in five different solvents, namely, DMSO, CH_3CN, EtOH, THF and $CHCl_3$ at 298 K (Figures S8–S13). Additionally, the emission solid state spectra were also obtained for these derivatives. The main results are summarized in Figure 1 and Table 1.

Table 1. Spectroscopic polarity parameters, physical properties of the different solvents. ε_r: relative permittivity; η: refractive index; α: the solvent's HBD acidity; β: the solvent´s HBA basicity; π*: the solvent´s dipolarity/polarizability.

Solvent	ε_r	α	β	π*	η
DMSO	47.24	0	0.76	1.00	1.47
CH_3CN	35.94	0.19	0.40	0.66	1.34
EtOH	24.30	0.86	0.75	0.54	1.36
THF	7.58	0	0.55	0.58	1.40
$CHCl_3$	4.89	0.20	0.10	0.69	1.44

Selecting acetonitrile as a representative solvent, all compounds exhibited an absorption band at 341 nm, 345 nm, 320 nm, 345 nm, 337 nm, 333 nm, from **L1** to **L6**, characteristic of the π - π* transition of the dansyl chromophores. These compounds appear colorless to the naked eye. However, upon emission, they display a pronounced yellow emission, with maximum bands at 519, 528, 535, 530, 520 and 528 nm, from **L1** to **L6**, respectively. Specifically, **L2**, **L3**, **L4** and **L6**, which have a benzene unit directly attached to the dansyl unit, do not exhibit significant changes were observed in the excited state, with maximum emission value ca. 528-530 nm. The same was not verified in the ground-state where the increase of donor atoms and side chain length promotes a red shift in the maximum bands, ranging from 320 nm to 345 nm. In contrast, **L1** and **L5**, which have a spacer between the dansyl chromophores, showed a blue shift of ca. 10 nm in the emission bands (*ca.* 519-520 nm), but no significant changes in the absorption.

For solid-state emissions, **L4** and **L5** produced emission bands at a longer wavelength (*ca.* 500-505 nm) than the other compounds (*ca.* 478-486 nm), probably due to their higher number of donor

Preprints (www.preprints.org) | NOT PEER-REVIEWED | Posted: 19 December 2023 doi:10.20944/preprints202312.1441.v1

atoms. **L1** and **L5** demonstrate the highest fluorescence quantum yield (ϕ =*ca.* 35-36%), suggesting that the introduction of a spacer might stabilize these molecules in their excited state.

An intriguing observation was the solvatochromic effect in various solvents. As solvent polarity increased, a change in emission color from yellow to green was noted. This change was due to a red shift in the maximum emission bands, varying from 496 to 522 nm for **L1**, 499 nm to 540 nm for **L2**, 503 to 536 nm for **L3**, 504 to 533 nm for **L4**, 500 nm to 524 nm to **L4** and 497 nm to 537 nm for **L6**, respectively. In the absorption no significant correlation is identified.

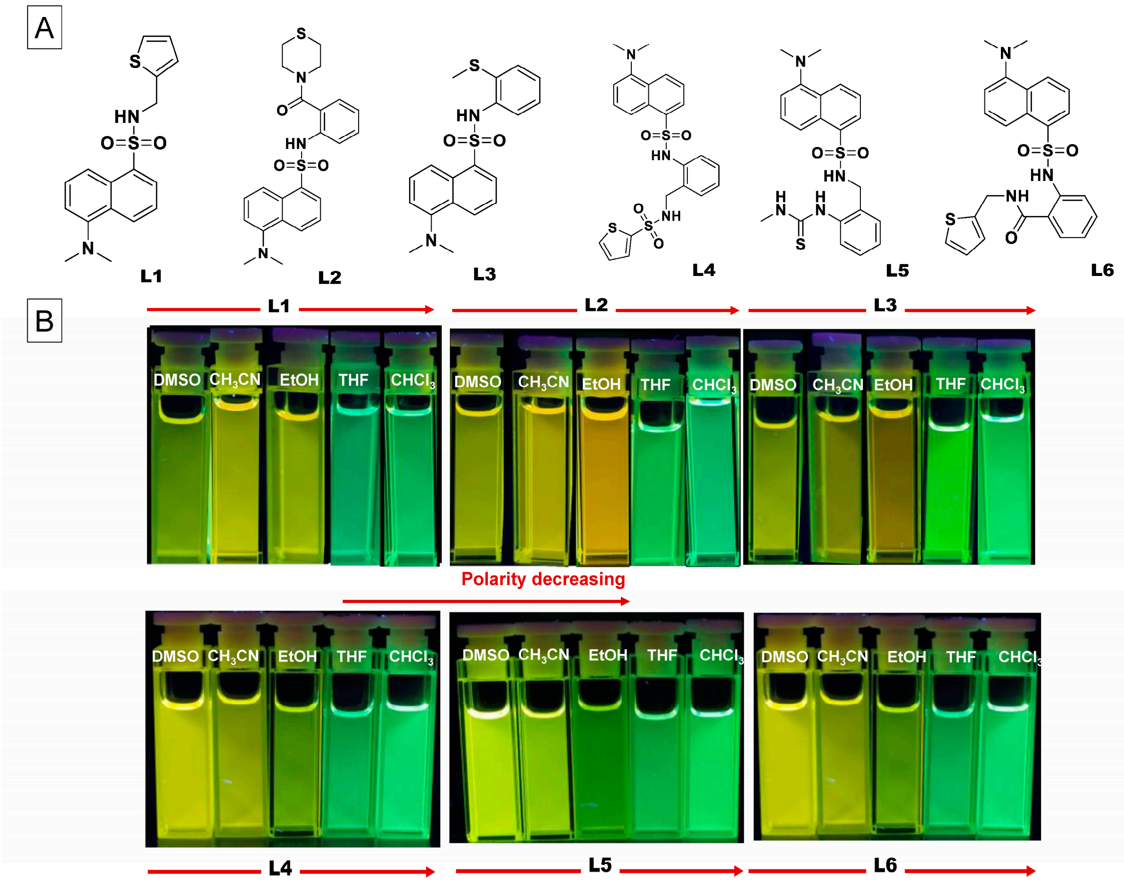

Figure 1. (A) Chemical structures of dansyl-derivatives **L1-L6**. (B) Images of **L1-L6** under a UV light lamp. Polarity decreasing from DMSO to $CHCl_3$.

Based on previous studies from our group it is evident that solvents with greater polarity significantly influence the stability of molecules. From the observed shifts, all compounds display a pronounced positive solvatochromic effect, suggesting enhanced stabilization of their excited state in highly polar solvents. This behavior provides an opportunity to stimulate the properties of the compound's microenvironment, offering potential applications in determining the local polarity in membranes, proteins, DNA [22]. Furthermore, this phenomenon can be valuable in understanding the characteristics of ionic liquids or mixed solvents and hold importance in the textile industry [23].

Table 2. Photophysical characterization data of dansyl derivatives **L1-L6** in the different solvents.

Cpd.	Solv.	λ_{abs} [nm]	λ_{em} [nm]	ε [10^3 cm^{-1} M^{-1}]	Stokes shift [cm^{-1}]	$\lambda_{em.solid}$ nm]	Φ (%)	Brightness (ε X ϕ) [cm^{-1} M^{-1}]	t[ns]
	DMSO	337	522	5.765	54054		22	1291	17
	CH_3CN	341	519	5.531	56179		35	1941	10
L1	EtOH	335	516	4.873	55248	484	31	1506	13
	THF	334	498	4.969	60975		21	1048	12
	$CHCl_3$	345	496	4.721	66225		35	1671	14

Preprints (www.preprints.org) | NOT PEER-REVIEWED | Posted: 19 December 2023 doi:10.20944/preprints202312.1441.v1

	DMSO	353	540	5.950	53475		11	666	13
	CH_3CN	345	528	5.519	54644		29	1606	12
L2	EtOH	346	520	4.983	57471	478	38	1913	13
	THF	334	504	5.201	58823		39	200	13
	$CHCl_3$	345	499	5.204	64935		37	1951	15
	DMSO	340	536	5.397	51020		10	550	13
	CH_3CN	320	535	5.454	46511		28	1538	11
L3	EtOH	340	531	5.052	52356	486	32	1596	11
	THF	339	511	4.921	58139		32	1555	13
	$CHCl_3$	346	503	4.057	63694		32	1282	15
	DMSO	343	533	4.254	52631		21	914	15
	CH_3CN	345	530	4.471	54054		27	1211	10
L4	EtOH	345	522	3.780	56497	505	17	646	13
	THF	343	502	4.653	62893		27	1261	13
	$CHCl_3$	345	504	4.482	62893		29	1313	15
	DMSO	339	524	4.640	54054		30	1378	17
	CH_3CN	337	520	5.674	54644		36	2048	11
L5	EtOH	338	515	3.968	56497	500	22	877	13
	THF	337	497	4.940	62500		26	1304	13
	$CHCl_3$	343	500	0.3593	63694		34	1210	15
	DMSO	347	537	4.279	52631		17	740	14
	CH_3CN	333	528	4.817	51282		28	1354	11
L6	EtOH	329	525	7.164	51020	486	17	1189	13
	THF	341	501	4.370	62500		29	1280	13
	$CHCl_3$	341	497	4.782	64102		34	1616	14

To quantitatively understand the interactions between solute and solvent, a multiparametric fit using the Kamlet-Taft equation was carried out (Equation 1). This equation enabled the determination of certain solute-dependent parameters which relate to solvent properties such as hydrogen bond donating (HBD) acidity (α), hydrogen bond accepting (HBA) basicity (β), and the solvent's dipolarity/polarizability (π^*).

$$\upsilon = \upsilon_0 + a\alpha + b\beta + p\pi^* \quad (1)$$

here υ_0 is the value of emission in a reference solvent. (see Table 1) [23].

Table 3 shows the fitted parameters (υ_0, a, b and p), the slope and correlation coefficients based on the fitting linear plots of $\upsilon_{exp.}$ versus υ_{calc}.

Table 3. υ_0, a, b and p-values, in cm^{-1}, slope and correlation coefficients obtained from Kamlet–Taft multiparametric fitting of the emission data.

	υ_0	a	b	p	Slope	R^2
L1	33032	-533	-4770	-17808	1.00	1
L2	35386	-350	-5804	-21300	1.00	1
L3	35354	-432	-6116	-21414	1.00	1
L4	35581	-638	-5444	-21838	1.00	1
L5	32841	-629	-4363	-17796	1.00	1
L6	36665	-672	-6248	-22877	1.00	1

Analysis of the results in Table 3, clearly evidences that the solvatochromic effect is essential due to higher sensitivity to H-bond acceptor (or electron donor) strength of the solvents, as can be observed in the b values, with one-order of magnitude higher than a, respectively. However, the values indicate an even stronger influence of the solvent's dipolarity/polarizability with p values with one and two orders of magnitude higher than a. Thus, electronic interactions (polarity and

Preprints (www.preprints.org) | NOT PEER-REVIEWED | Posted: 19 December 2023 doi:10.20944/preprints202312.1441.v1

polarizability) and hydrogen bond accepting behavior of the solvent play a dominant role compared to its hydrogen bond donating character.

3.3. Metal sensing ability

The sensorial ability of dansyl derivatives **L1-L6** towards Zn^{2+}, Cu^{2+}, Hg^{2+}, Ag^{+} metal ions in acetonitrile, was evaluated by titrating the free ligand with small amounts of the metal ions. The absorption and emission spectra were collected at 298 K until reaching a plateau. From all studied metal ions, all dansyl derivatives showed to only sense Cu^{2+} and Hg^{2+} metal ions, as already verified in our previous studies [5,6]. The spectral behavior was quite similar between ligands, thus as a representative example the dansyl derivatives **L1** and **L5** were selected. **L5** despite less intensive also revealed sensibility to Ag^{+} metal ions. Titrations with the other ligands are presented in Supplementary Material (Figures S14–S18). Figure 2 shows the absorption and emission spectral changes of **L1** upon coordination with Cu^{2+} metal ions, in acetonitrile. When increasing of Cu^{2+} and Hg^{2+} concentration similar spectral behavior in the absorption is noticed, resulting on a decrease in the absorption at 341 nm from both, and an increase in the absorbance at 298 nm and 287 nm for Cu^{2+} and Hg^{2+}, respectively. The emission spectra a fast decrease in the emission intensity at 519 nm is detected in both cases. Cu^{2+} metal ions, as a paramagnetic transition metal ion has unfilled *d* orbital shells. This characteristic makes it particularly susceptible to the chelation enhancement of quenching (CHEQ effect). The causing mechanisms driving this effect can be electron transfer or energy transfer.

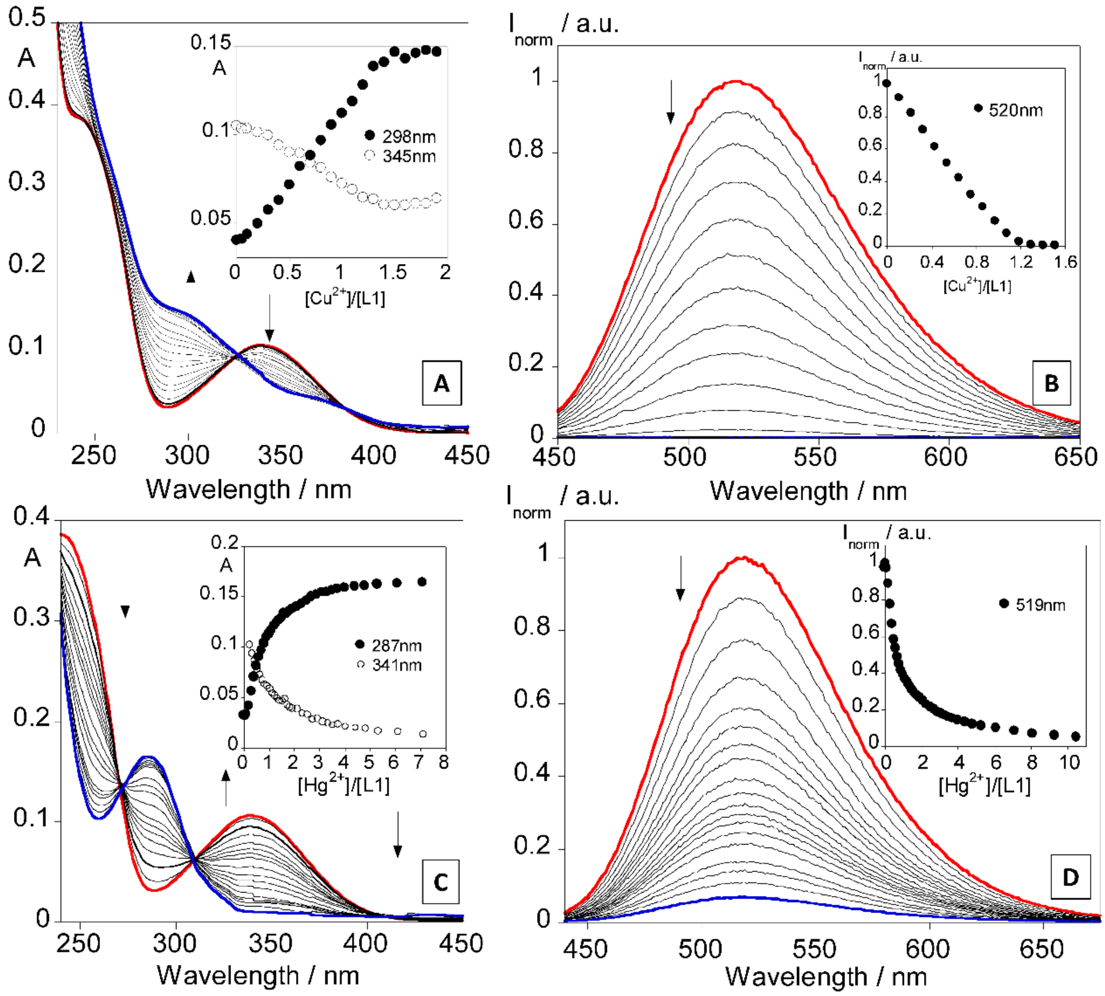

Figure 2. Spectrophotometric and spectrofluorometric titrations of dansyl derivative **L1** with increased additions of Cu^{2+} (A, B), and Hg^{2+} (C, D) in CH_3CN. The inset represents the absorption (A, C) and emission (B-D) as a function of $[Cu^{2+}]/[\mathbf{L1}]$ and $[Hg^{2+}]/[\mathbf{L1}]$, respectively. $[\mathbf{L1}] = 20\ \mu M$, $\lambda_{excL1}=341$ nm, T = 298 K).

Preprints (www.preprints.org) | NOT PEER-REVIEWED | Posted: 19 December 2023 doi:10.20944/preprints202312.1441.v1

Conversely, Hg^{2+} presents a unique case. While it is a diamagnetic metal with a filled d^{10} configuration, its quenching behaviour is not analogous to typical diamagnetic ions. The primary reason could be Spin-Orbit coupling due to its large atomic number, causing more predominant non-radiative deactivation pathways, which can also be induced by the formation of heavy atom complexes [24–26].

Figure 3 presents the absorption and emission titrations of **L5** in response to the addition of Cu^{2+}, Hg^{2+} and Ag^{+} metal ions. The spectral patterns observed are consistent with those seen for the other ligands, with a notable exception for Ag^{+} where a quenching in the emission intensity is also detected. In this case, no spectral changes were observed in the ground state. The observed emission quenching can be attributed probably to the photoinduced electron transfer effect induced by Ag^{+}, which is consistent with the **L5** structure where the number of nitrogen atoms is higher.

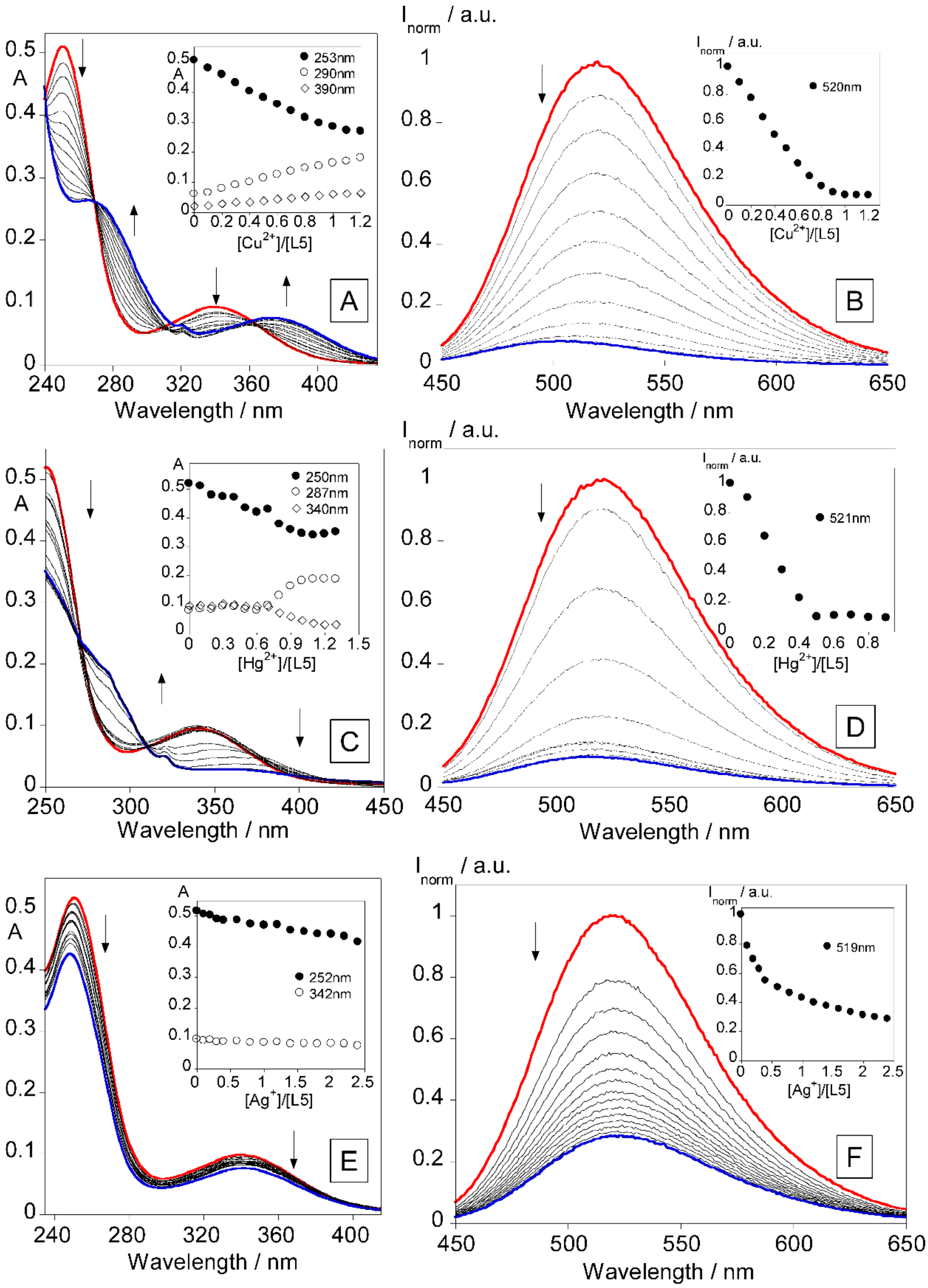

Preprints (www.preprints.org) | NOT PEER-REVIEWED | Posted: 19 December 2023 doi:10.20944/preprints202312.1441.v1

Figure 3. Spectrophotometric and spectrofluorometric titrations of dansyl derivative **L5** with increased additions of Cu^{2+} (A, B), Hg^{2+} (C, D), and Ag^{+} (E, F) in CH_3CN. The inset represents the absorption (A, C) and emission (B-D) as a function of [Cu^{2+}]/[**L1**] and [Hg^{2+}]/[**L1**], respectively. [**L1**] = 20 μM, λ_{excL2}=337 nm, T = 298 K).

In order to provide more insights into the interactions between the dansyl derivatives **L1-L6** with the tested metal ions and quantify the strength of these interactions, their stability constants were determined using the HypSpec program [10]. The summarized results are presented in Table 4.

Table 4. Stability association constants and stoichiometry for the complexes formed from **L1** to **L6** with Cu^{2+}, Hg^{2+}, Ag^{+} ions, in CH_3CN.

Compounds (L)	Metal (M)	Association constants ($LogK_{ass.}$)	L:M
L1	Cu^{2+}	7.22±0.06	1:1
	Hg^{2+}	9.10±0.01	1:1
L2	Cu^{2+}	10.54±0.01	1:1
	Hg^{2+}	8.96±0.01	1:1
L3	Cu^{2+}	11.40±0.02	1:1
	Hg^{2+}	9.44±0.01	1:1
L4	Cu^{2+}	5.34±0.01	1:1
	Hg^{2+}	5.76±0.01	1:1
L5	Cu^{2+}	5.92±0.01	1:1
	Hg^{2+}	5.20±0.01	1:1
	Ag^{+}	5.30±0.01	1:1
L6	Cu^{2+}	7.15±0.02	1:1
	Hg^{2+}	5.67±0.01	1:1

The stability constants indicate the formation of mononuclear species for Cu^{2+} and Hg^{2+} in the case of **L1-L6** and also for Ag^{+} in the case of compound **L5**. Notably, **L3** exhibits the highest stability constant among the derivatives with a value of $LogK_{ass.}$ = 11.40±0.02 for its interaction with Hg^{2+}. We can observe that compounds **L1**, **L2**, and **L3** exhibit higher stability constants towards Cu^{2+} and Hg^{2+} than compounds **L4**, **L5** and **L6**. These results are in agreement with other dansyl derivatives studied previously in our group, being Hg^{2+} or Cu^{2+} the higher values observed.

The acid-base properties of all dansyl derivatives were also evaluated. While consistent results were observed across all compounds, Figure 4 specifically depicts the behavior of **L1** when treated with HCl and ammonia. Detailed results for the other derivatives are available in the Supplementary Material (Figures S19-S22). The addition of acid produces a decrease in the absorption at 345 nm, as well as, in the emission intensity at 519 nm. Conversely, when ammonia is added, the opposite is observed with an increase in the absorption band at 345 nm, which is accompanied by a rise, ca. 60% in the emission intensity of **L1**.

Having in mind these results, the acid-base responsive dansyl derivatives were introduced into PMMA polymers offering several applications, such as environmental.

Preprints (www.preprints.org) | NOT PEER-REVIEWED | Posted: 19 December 2023 doi:10.20944/preprints202312.1441.v1

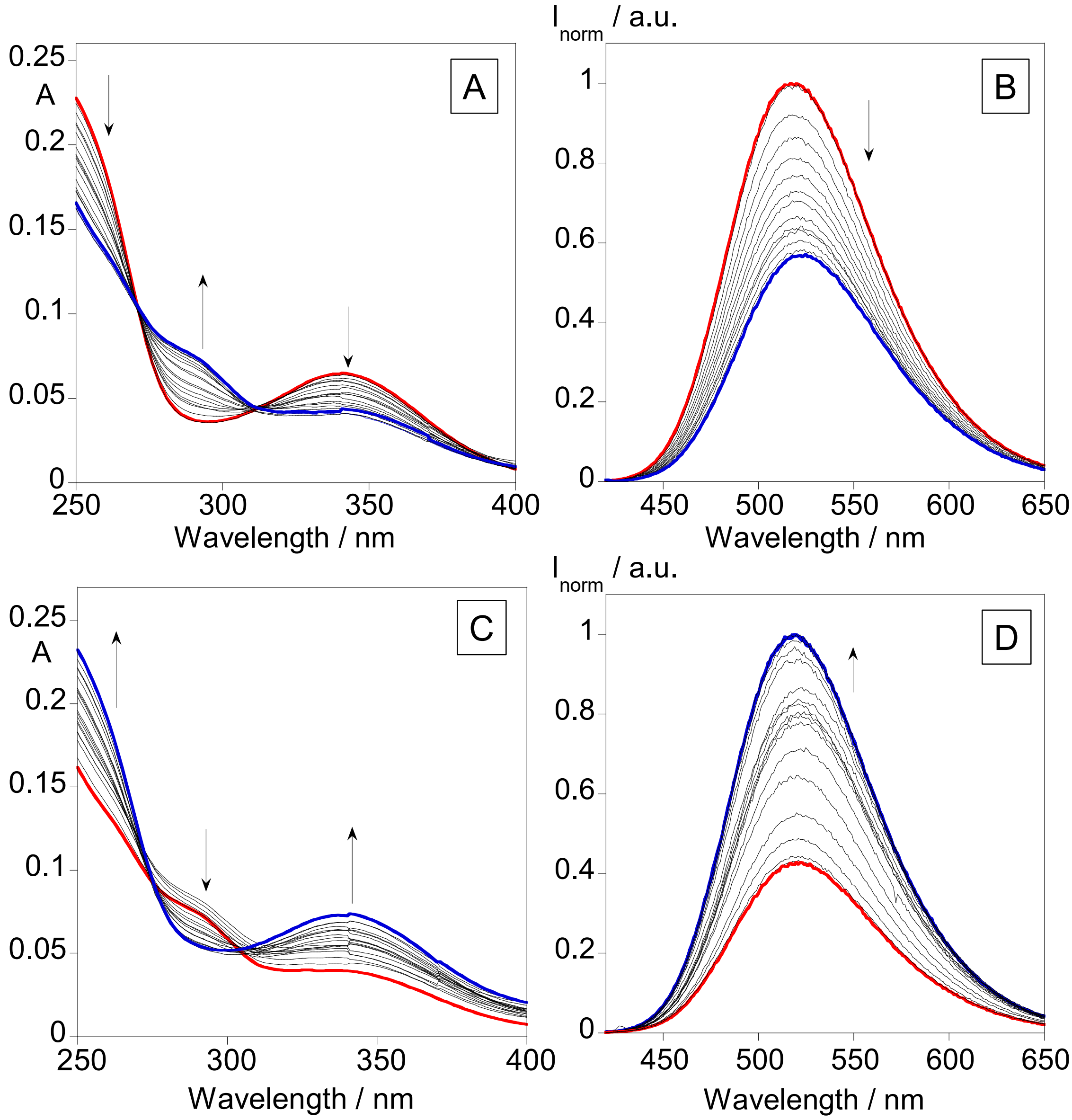

Figure 4. Spectrophotometric and spectrofluorometric titrations of dansyl derivative **L1** with increased additions of HCl (A, B), and ammonia in CH_3CN. [**L1**] = 20 μM, λ_{excL1}=345 nm, T = 298 K).

3.4. Low-cost dye-doped PMMA polymers: detection of acidic environments

Incorporation of acid-base responsive dansyl derivatives into polymers can transform them into smart, adaptive materials with a broad range of potential applications in sensing, electronic, healthcare, among others. The creation of a polymer acid-base sensitive to environment can be crucial in applications where pH monitoring or sensing is essential.

PMMA polymers doped with compounds **L1**-**L6** were successfully synthetized. All doped polymers from **L1** to **L6**, except for **L5**, showed to be sensitive to acid-base environment (see Supplementary Material: Figure S23). Figure 5 shows the results obtained for **L1**, as a representative case. As the first approach, the **L1**@PMMA polymer was immersed into a concentrated solution of HCl, and at each 5 minutes an emission spectrum was recorded. Afterwards, other polymer was submitted to HCl vapours, and the emission spectra taken at each 20 minutes. The doped polymers have all an initial strong blue emission, which was progressively decreasing in both acidic environments. It is interesting to note, that in solution in general all compounds have a green emission, but when incorporated into a PMMA such emission suffers a blue shift, emitting consequently a blue color. As previously seen these compounds are highly influenced by the

Preprints (www.preprints.org) | NOT PEER-REVIEWED | Posted: 19 December 2023 doi:10.20944/preprints202312.1441.v1

surrounding solvent molecules, affecting their electronic properties. In a solid polymer matrix, the local environment is different, the polymer is a more rigid structure causing changes in the molecular conformation or restricting the rotational and vibrations of the molecule, affecting the electronic transitions and thus its emission wavelength.

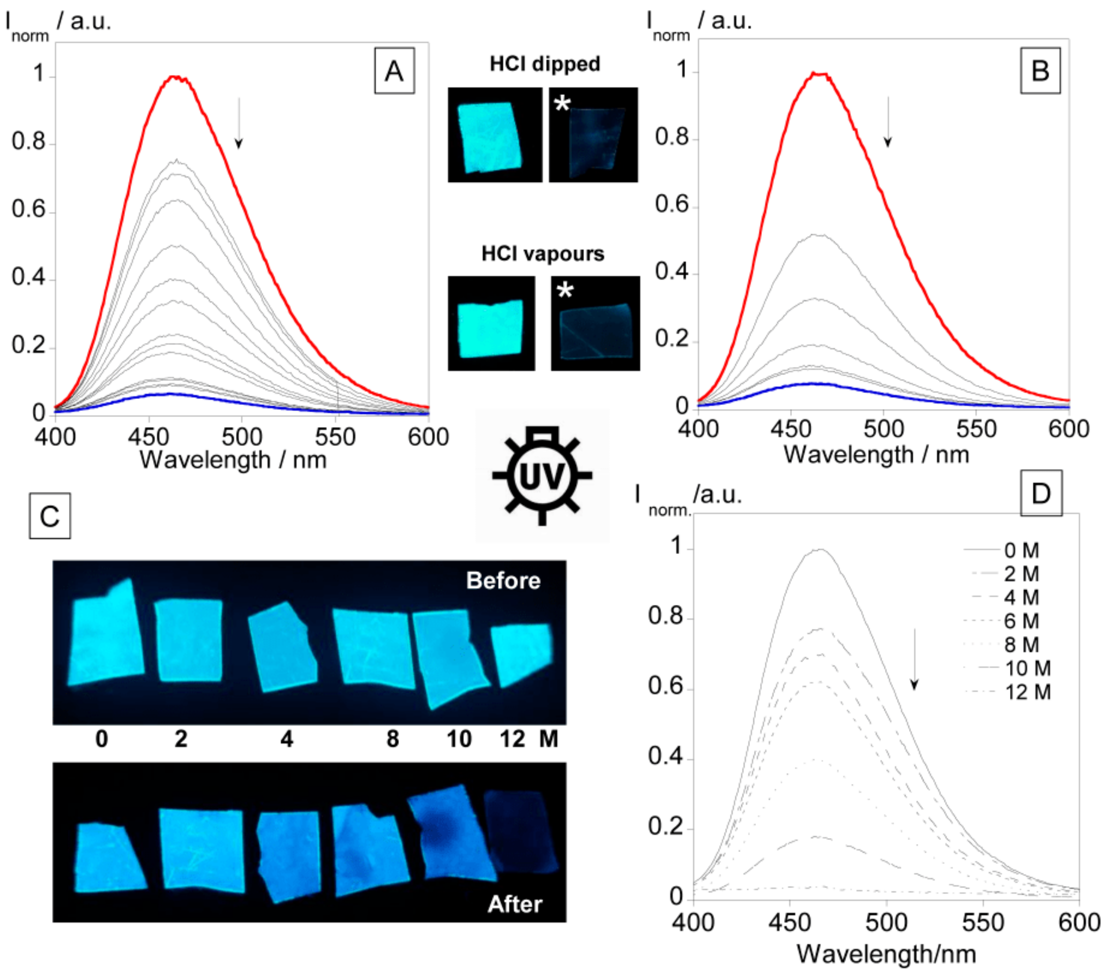

Figure 5. (A) Emission spectra of successive immersion of **L1** doped PMMA polymer film in a concentrated HCl solution (5m in 5min). (B) Emission spectra of exposure of **L1** to HCl vapours (20m in 20m), T = 298 K. Images under a UV lamp (C) and emission spectra (D) of **L1** immersion in the HCl concentrations from 0 to 12 M, λ_{excL1}=345nm.

In the second approach, the doped polymers were dipped in a 2-12 M gradient of HCl solutions (Figures 5 C,D and S24). By emission, it is possible to verify the doped polymer response at the lowest HCl concentration 2 M, with a reduction in the emission signal of ca. 25%. Visually under a UV lamp, a result is verified after 4 M, with a total absence of emission at 12 M. The reproducibility of the dye-doped polymers was proved by continuous emersion of the polymers in HCl and ammonia for different cycles (See Supplementary Material: Figure S25).

4. Conclusions

The synthesis and characterization of six dansyl derivatives have led to the creation of innovative sensing materials when incorporated into PMMA polymers. These compounds exhibited a positive solvatochromic effect, causing a shift in emission colour from yellow to green as solvent polarity increased, accompanied by red-shifts of 30-40nm in emission maximum wavelength. The studies towards metal ions revealed the sensitivity of these compounds to Cu^{2+} and Hg^{2+}, with complete emission intensity quenching upon the addition of no more than 2 equivalents of each metal. The acid-sensing studies conducted showed that all six compounds, except **L3**, hold substantial potential for developing cost-effective systems to detect acidic environments. They displayed significant emission intensity quenching and recovery when titrated with HCl and NH_3, respectively, in solution. In PMMA polymer matrices, gradual intensity reductions were observed after successive immersions in HCl and exposure to HCl vapours, and these systems exhibited good emission intensity reversibility after ten cycles, underscoring their reusability.

Thus, these materials demonstrate a potent combination of solvatochromism, selective metal ion sensing, and acid-base responsiveness. Moreover, this work highlights the compounds' sensitivity to environmental changes, particularly in detecting metal ions and pH variations.

The integration into polymers not only enhances the practical utility of the dansyl derivatives but also opens new avenues for their application in environmental monitoring and bioanalytical chemistry. Future work could explore further functionalization to enhance their sensitivity and selectivity, paving the way for more robust and versatile sensing platforms.

Supplementary Materials: Supplementary material regarding compounds' physical and photophysical characterization, sensing ability towards metal ions, acid-base titrations, and sensorial ability of dye-doped polymers with acids and bases can be downloaded at the website of this paper posted on Preprints.org.

Author Contributions: Conceptualization, GMD, EO and CL; methodology, GMD, EO and CL; validation, GMD, AK, EO and CL; formal analysis, GP, GMD, AK, HMS, EO and CL; investigation, GP, FD, [GMD, AK (synthesis of the compounds)], HMS (mass spectrometry analysis), EO and CL; resources, GMD, AK, HMS, JLC-M, EO and CL; writing—original draft preparation, GP and EO; writing—review and editing, GP, GMD, AK, EO and CL; supervision, GMD, EO and CL; funding acquisition, GMD, AK, HMS, JLC-M, EO and CL. All authors have read and agreed to the published version of the manuscript.

Funding: This work was supported by the Associate Laboratory for Green Chemistry - LAQV which is financed by national funds from FCT/MCTES (UIDB/50006/2020 and UIDP/50006/2020) as well as the Scientific Society PROTEOMASS (Portugal) for funding support (General Funding Grant). F.D. thanks FCT/MEC (Portugal) for his doctoral grant 2021.05161.BD. E.O thanks FCT/MEC (Portugal) for the individual contract, CEECIND/05280/2022. HMS acknowledges the Associate Laboratory for Green Chemistry-LAQV (LA/P/0008/2020) funded by FCT/MCTES for his research contract. The financial support by the Bulgarian National Science Fund (BNSF) under grant – "Novel styryl and polymethine fluorophores as potential theranostic agents "contract N◦ KΠ-06-M59/1 from 15.11.2021 is gratefully acknowledged by A.K. This work is also developed and acknowledged by A.K. as part of contract N◦: BG-RRP-2.004-0002-C01, Laboratory of Organic Functional Materials (Project BiOrgaMCT), Procedure BG-RRP-2.004, Establishing of a network of research higher education institutions in Bulgaria", funded by BULGARIAN NATIONAL RECOVERY AND RESILIENCE PLAN". G.D. thanks to the European Regional Development Fund within the Operational Programme Science and Education for Smart Growth 2014 - 2020 under the ProJect Center of Exellence: National center of mechatronics and clean technologies - BG05M2OP001-1.001-0008 for the financial support.

Data Availability Statement: Not applicable.

Conflicts of Interest: The authors declare no conflict of interest.

References

1. Sivaraman, G.; Iniya, M.; Anand, T.; Kotla, N.G.; Sunnapu, O.; Singaravadivel, S.; Gulyani, A.; Chellappa, D. Chemically Diverse Small Molecule Fluorescent Chemosensors for Copper Ion. *Coord Chem Rev* **2018**, *357*, 50–104. https://doi.org/10.1016/j.ccr.2017.11.020.
2. Oliveira, E.; Bértolo, E.; Núñez, C.; Pilla, V.; Santos, H.M.; Fernández-Lodeiro, J.; Fernández-Lodeiro, A.; Djafari, J.; Capelo, J.L.; Lodeiro, C. Green and Red Fluorescent Dyes for Translational Applications in Imaging and Sensing Analytes: A Dual-Color Flag. *ChemistryOpen* **2017**. https://doi.org/10.1002/open.201700167.
3. Qin, X.; Yang, X.; Du, L.; Li, M. Polarity-Based Fluorescence Probes: Properties and Applications. *RSC Med Chem* **2021**, *12*, 1826–1838. https://doi.org/10.1039/D1MD00170A.
4. Wei, P.; Xiao, L.; Gou, Y.; He, F.; Zhou, D.; Liu, Y.; Xu, B.; Wang, P.; Zhou, Y. Fluorescent "on–off–on" Probe Based on Copper Peptide Backbone for Specific Detection of Cu(II) and Hydrogen Sulfide and Its Applications in Cell Imaging, Real Water Samples and Test Strips. *Microchemical Journal* **2022**, *182*, 107848. https://doi.org/10.1016/j.microc.2022.107848.

5. Duarte, F.; Dobrikov, G.; Kurutos, A.; Santos, H.M.; Fernández-Lodeiro, J.; Capelo-Martinez, J.L.; Oliveira, E.; Lodeiro, C. Enhancing Water Sensing via Aggregation-Induced Emission (AIE) and Solvatofluorochromic Studies Using Two New Dansyl Derivatives Containing a Disulfide Bound: Pollutant Metal Ions Detection and Preparation of Water-Soluble Fluorescent Polymeric Particles. *Dyes and Pigments* **2023**, *218*, 111428. https://doi.org/10.1016/j.dyepig.2023.111428.
6. Duarte, F.; Dobrikov, G.; Kurutos, A.; Capelo-Martinez, J.L.; Santos, H.M.; Oliveira, E.; Lodeiro, C. Development of Fluorochromic Polymer Doped Materials as Platforms for Temperature Sensing Using Three Dansyl Derivatives Bearing a Sulfur Bridge. *J Photochem Photobiol A Chem* **2023**, *445*, 115033. https://doi.org/10.1016/j.jphotochem.2023.115033.
7. Métivier, R.; Leray, I.; Lebeau, B.; Valeur, B. A Mesoporous Silica Functionalized by a Covalently Bound Calixarene-Based Fluoroionophore for Selective Optical Sensing of Mercury(Ii) in Water. *J Mater Chem* **2005**, *15*, 2965. https://doi.org/10.1039/b501897h.
8. Algethami, J.S. A Review on Recent Progress in Organic Fluorimetric and Colorimetric Chemosensors for the Detection of $Cr^{3+/6+}$ Ions. *Crit Rev Anal Chem* **2022**, 1–21. https://doi.org/10.1080/10408347.2022.2082242.
9. Adhikari, B.; Majumdar, S. Polymers in Sensor Applications. *Prog Polym Sci* **2004**, *29*, 699–766. https://doi.org/10.1016/j.progpolymsci.2004.03.002.
10. GANS, P.; SABATINI, A.; VACCA, A. Investigation of Equilibria in Solution. Determination of Equilibrium Constants with the HYPERQUAD Suite of Programs. *Talanta* **1996**, *43*, 1739–1753. https://doi.org/10.1016/0039-9140(96)01958-3.
11. Berlman, I.B.; I. B. Berlman; Berlman, I.B. *Handbook of Fluorescence Spectra of Aromatic Molecules*; Press, A., Ed.; 2nd ed.; Academic Press, NY: New York, 1971;
12. M. Montalti, A. Credi, L. Prodi, M.G.; Montalti M, Credi A, Prodi L, G.M. *Handbook of Photochemistry*; 3rd Ed. Taylor & Francis, B.Raton., Ed.; 3rd ed.; Taylor & Francis, Boca Raton: BOCA, 2006;
13. Shi, F.; Tse, M.K.; Zhou, S.; Pohl, M.-M.; Radnik, J.; Hübner, S.; Jähnisch, K.; Brückner, A.; Beller, M. Green and Efficient Synthesis of Sulfonamides Catalyzed by Nano-Ru/Fe_3O_4. *J Am Chem Soc* **2009**, *131*, 1775–1779. https://doi.org/10.1021/ja807681v.
14. Yang, Y.; Yu, X.; He, N.; Huang, X.; Song, X.; Chen, J.; Lin, J.; Jin, Y. $FeCl_3$-Catalyzed Oxidative Amidation of Benzylic C–H Bonds Enabled by a Photogenerated Chlorine-Radical. *Chemical Communications* **2023**, *59*, 10299–10302. https://doi.org/10.1039/D3CC03186A.
15. Huang, F.-Q.; Dong, X.; Qi, L.-W.; Zhang, B. Visible-Light Photocatalytic α-Amino C(Sp3)–H Activation through Radical Translocation: A Novel and Metal-Free Approach to α-Alkoxybenzamides. *Tetrahedron Lett* **2016**, *57*, 1600–1604. https://doi.org/10.1016/j.tetlet.2016.02.108.
16. Ye, W.; Liu, Y.; Ren, Q.; Liao, T.; Chen, Y.; Chen, D.; Wang, S.; Yao, L.; Jia, Y.; Zhao, C.; et al. Design, Synthesis and Biological Evaluation of Novel Triazoloquinazolinone and Imidazoquinazolinone Derivatives as Allosteric Inhibitors of SHP2 Phosphatase. *J Enzyme Inhib Med Chem* **2022**, *37*, 1495–1513. https://doi.org/10.1080/14756366.2022.2078968.
17. Tang, B.-D.; Zhang, J.-Y.; Ma, H.-X.; Wang, N.; An, X.; Li, G.-M.; Zhou, Z. SYNTHESIS, CRYSTAL STRUCTURE, AND DFT STUDY OF 1-(PYRROLIDIN-1- YL-METHYL)-4-(THIOPHEN-2-YL-METHYL)-[1,2,4]TRIAZOLO[4,3-a]QUINAZOLIN-5(4H)-ONE. *Journal of Structural Chemistry* **2022**, *63*, 19–25. https://doi.org/10.1134/S0022476622010036.
18. Zaytsev, V.P.; Revutskaya, E.L.; Kuz´menko, M.G.; Novikov, R.A.; Zubkov, F.I.; Sorokina, E.A.; Nikitina, E. V.; Toze, F.A.A.; Varlamov, A. V. Synthesis of Furyl-, Furylvinyl-, Thienyl-, Pyrrolinylquinazolines and Isoindolo[2,1-a]Quinazolines. *Russian Chemical Bulletin* **2015**, *64*, 1345–1353. https://doi.org/10.1007/s11172-015-1016-1.
19. Jang, Y.; Lee, S.B.; Hong, J.; Chun, S.; Lee, J.; Hong, S. Synthesis of 2-Aryl Quinazolinones *via* Iron-Catalyzed Cross-Dehydrogenative Coupling (CDC) between N–H and C–H Bonds. *Org Biomol Chem* **2020**, *18*, 5435–5441. https://doi.org/10.1039/D0OB00866D.
20. Sanmartín-Matalobos, J.; Bermejo-Barrera, P.; Pérez-Juste, I.; Fondo, M.; García-Deibe, A.M.; Alves-Iglesias, Y. Experimental and Computational Studies on the Interaction of a Dansyl-Based Fluorescent Schiff Base Ligand with Cu2+ Ions and CuO NPs. *Int J Mol Sci* **2022**, *23*, 11565. https://doi.org/10.3390/ijms231911565.
21. Ambati, N.B.; Anand, V.; Hanumanthu, P. A Facile Synthesis of 2-N(Methyl Amino) Benzothiazoles. *Synth Commun* **1997**, *27*, 1487–1493. https://doi.org/10.1080/00397919708006084.
22. Aliaga-Alcalde, N.; Rodríguez, L. Solvatochromic Studies of a Novel Cd2+–Anthracene-Based Curcuminoid and Related Complexes. *Inorganica Chim Acta* **2012**, *380*, 187–193. https://doi.org/10.1016/j.ica.2011.08.052.
23. Elisabete oliveira, Rosa M. F. Baptista, Susana P. G. Costa, M. Manuela M. Raposo, C.L. Synthesis and Solvatochromism Studies of Novel Bis(Indolyl)Methanes Bearing Functionalized Arylthiophene Groups as New Colored Materials. *Photochemical & Photobiological Sciences* **2014**, *13*, 492–498. https://doi.org/10.1039/c3pp50352f.
24. Marcelo, G.A.; Pires, S.M.G.; Faustino, M.A.F.; Simões, M.M.Q.; Neves, M.G.P.M.S.; Santos, H.M.; Capelo, J.L.; Mota, J.P.; Lodeiro, C.; Oliveira, E. New Dual Colorimetric/Fluorimetric Probes for Hg2+ Detection

& Extraction Based on Mesoporous SBA-16 Nanoparticles Containing Porphyrin or Rhodamine Chromophores. *Dyes and Pigments* **2019**, *161*, 427–437. https://doi.org/10.1016/j.dyepig.2018.09.068.

25. Gonc, A.C.; Luis, J.; Lodeiro, C.; Dos, A.A. Sensors and Actuators B : Chemical A Seleno-Pyrene Selective Probe for Hg 2 + Detection in Either Aqueous or Aprotic Systems. **2017**, *239*, 311–318. https://doi.org/10.1016/j.snb.2016.08.014.
26. Pinheiro, D.; De Castro, C.S.; Seixas De Melo, J.S.; Oliveira, E.; Nu??ez, C.; Fern??ndez-Lodeiro, A.; Capelo, J.L.; Lodeiro, C. From Yellow to Pink Using a Fluorimetric and Colorimetric Pyrene Derivative and Mercury (II) Ions. *Dyes and Pigments* **2014**, *110*, 152–158. https://doi.org/10.1016/j.dyepig.2014.04.012.